

Synthesis and Structures of Cycloalkylidene-Bridged Cyclopentadienyl Metallocene Catalysts: Effects of the Bridges of Ansa-Metallocene Complexes on the Catalytic Activity for Ethylene Polymerization

Baiquan Wang,^{*,[a]} Bin Mu,^[a] Xiaobin Deng,^[a] Huiling Cui,^[a] Shansheng Xu,^[a] Xiuzhong Zhou,^[a] Fenglou Zou,^[b] Yang Li,^[b] Ling Yang,^[c] Yufei Li,^[c] and Youliang Hu^[c]

Abstract: A series of cycloalkylidene-bridged cyclopentadienyl metallocene complexes, $[(CH_2)_n C(C_5H_4)_2 MCl_2]$ ($M = Ti$, $n = 4$ (**4**), 5 (**5**), 6 (**6**); $M = Zr$, $n = 4$ (**7**), 5 (**8**), 6 (**9**); $M = Hf$, $n = 4$ (**10**), 5 (**11**), 6 (**12**)), have been synthesized and applied to ethylene polymerization after activation with methyl aluminoxane (MAO). The cycloalkylidene-bridged titanocene catalysts exhibit much higher activities than the corresponding zirconocene and hafno-

cene analogues, and have the highest activities at higher temperatures. In comparison, the silacyclopentylidene-bridged metallocene complexes $[(CH_2)_4 Si(C_5H_4)_2 MCl_2]$ ($M = Ti$ (**13**), Zr (**14**)) and isopropylene-bridged metallocene complexes $[Me_2 C(C_5H_4)_2 MCl_2]$

($M = Ti$ (**15**), Zr (**16**)) have also been synthesized and applied to ethylene polymerization. In both cases, the titanocene complexes show much higher activities than the corresponding zirconocene analogues, especially at a lower temperature. The molecular structures of complexes **4–9** have been determined by X-ray diffraction. The structure–activity relationships, especially the effects of the bridges of ansa-metallocene complexes, are discussed.

Keywords: bridging ligands • metallocenes • structure–activity relationships • titanium • zirconium

Introduction

Metallocene catalysts have been one of the most actively investigated research topics for more than 20 years.^[1–3] Studies of various ring-bridged cyclopentadienyl and indenyl metallocene complexes have demonstrated that the activity and the stereoselectivity of olefin polymerization reactions can be significantly affected by slight structural variations of the bridging groups and ring substituents in metallocene catalysts.^[3] The Latin prefix *ansa* (to denote the presence of an

interannular bridge in metallocene complexes) was introduced by Brintzinger, who pioneered the design and synthesis of these complexes.^[4] Since Kaminsky and Brintzinger reported that the C_2 -symmetric ansa-zirconocene complex, racemic $[C_2H_4(1-IndH_4)_2 ZrCl_2]$ ($IndH_4$ = tetrahydroindenyl) activated with methyl aluminoxane (MAO) produced highly isotactic polypropylene,^[5] many Group 4 ansa-metallocene complexes have been developed and applied as olefin polymerization catalysts.^[2,6] Shapiro concluded that the functions of the ansa bridge in metallocene complex chemistry^[7] include: a) fixing the symmetry of the metallocene complex by preventing free rotation of the rings; b) controlling the stereochemistry of metallocene complex formation by directing the orientation of the rings upon metalation; c) influencing the reactivity of the metal by enforcing a bent-sandwich geometry between the rings; d) increasing the electrophilicity of the metal and increasing the access of substances to the equatorial wedge of the complex by increasing the tilt of the rings on the metal; and e) providing a reactive site at which ring-opening polymerization chemistry, ligand substitution, reversible bridge formation, and reversible metal ion bonding can occur.

In recent years, a number of ansa-metallocene complexes have also been synthesized and applied to olefin polymeri-

[a] Prof. B. Wang, B. Mu, X. Deng, H. Cui, Prof. S. Xu, Prof. X. Zhou
The State Key Laboratory of Elemento-Organic Chemistry
Department of Chemistry, Nankai University
Tianjin 300071 (P. R. China)
Fax: (+86) 22-235-02458
E-mail: bqwang@nankai.edu.cn

[b] F. Zou, Dr. Y. Li
Research Institute of Beijing Yanshan Petrochemical Corporation, SINOPEC
Beijing 102550 (P. R. China)

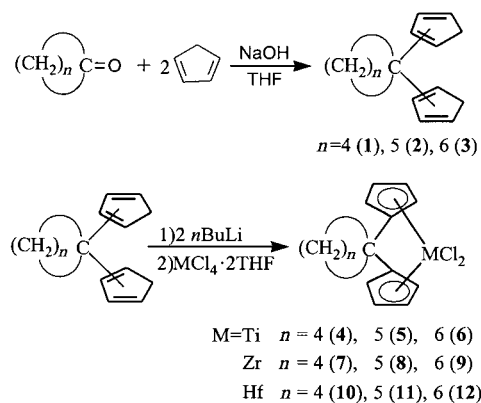
[c] L. Yang, Prof. Y. Li, Prof. Y. Hu
Institute of Chemistry, Chinese Academy of Science
Beijing 100080 (P. R. China)

zation by our group.^[8,9] We have reported that the cycloalkylidene-bridged titanocenes show much higher activities than zirconocenes and hafnocenes for ethylene polymerization.^[9] This is very different from the general recognition that zirconocene catalysts exhibit higher activities than titanocenes and hafnocenes in olefin polymerization.^[2,3,8] To study further the structural factors affecting the catalytic activities, we now report the synthesis and structures of a series of cycloalkylidene-bridged cyclopentadienyl Group 4 metallocene complexes $[(CH_2)_n C(C_5H_4)_2 MCl_2]$ ($M = Ti$, $n = 4$ (**4**), 5 (**5**), 6 (**6**); $M = Zr$, $n = 4$ (**7**), 5 (**8**), 6 (**9**); $M = Hf$, $n = 4$ (**10**), 5 (**11**), 6 (**12**)). To focus on the effects of the bridges of ansa-metallocene complexes on the catalytic activity for ethylene polymerization, the silacyclopentylidene-bridged metallocene complexes $[(CH_2)_4 Si(C_5H_4)_2 MCl_2]$ ($M = Ti$ (**13**), Zr (**14**)), and isopropylene-bridged metallocene complexes $[Me_2C(C_5H_4)_2 MCl_2]$ ($M = Ti$ (**15**), Zr (**16**)) have also been synthesized and applied to ethylene polymerization. In all cases, the titanocene complexes show much higher activities than the corresponding zirconocene analogues, especially at a lower temperature. The structure–activity relationships, especially the effects of the bridges of ansa-metallocene complexes, are discussed.

Results and Discussion

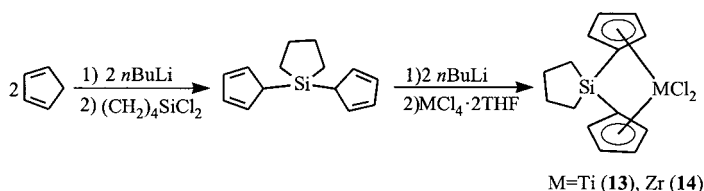
Synthesis of complexes $(CH_2)_n C(C_5H_4)_2 MCl_2$ (4**–**12**):** Cycloalkylidene-bridged biscyclopentadiene (1,1-biscyclopentadienylcycloalkane) ligands **1** and **2** were synthesized by reaction of cyclopentadiene with cyclopentanone and cyclohexanone in NaOH–THF according to literature methods,^[10] and **3** was synthesized from cyclopentadiene and cycloheptanone similarly. Ligands **1**–**3** were treated with $nBuLi$ and then reacted with $MCl_4 \cdot 2THF$ to give the cycloalkylidene-bridged metallocene complexes $[(CH_2)_n C(C_5H_4)_2 MCl_2]$ (**4**–**12**) (Scheme 1).

Synthesis of complexes $[(CH_2)_4 Si(C_5H_4)_2 MCl_2]$ (13**, **14**):** To study the effects of the bridges of ansa-metallocene complexes further, the silacyclopentylidene-bridged metallocene complexes **13** and **14** were synthesized for comparison. Cyclotetramethylenedichlorosilane, $(CH_2)_4 SiCl_2$, reacted with cyclopentadienyllithium to give the 1,1-biscyclopentadienyl-



Scheme 1. Synthesis of complexes $[(CH_2)_n C(C_5H_4)_2 MCl_2]$.

1-silacyclopentane ligand $(CH_2)_4 Si(C_5H_5)_2$, which, without separation, further reacted with $nBuLi$ and $TiCl_4 \cdot 2THF$ or $ZrCl_4 \cdot 2THF$ to yield complexes **13** and **14** (Scheme 2).



Scheme 2. Synthesis of complexes $[(CH_2)_4 Si(C_5H_4)_2 MCl_2]$.

The 1H NMR spectra of complexes **4**–**14** are consistent with their composition and structures. The α -H and β -H of $(\eta^5-C_5H_4)$ show two multiplets resulting from an A_2B_2 or $AA'BB'$ splitting pattern for these complexes. For the cycloalkylidene bridged complexes, the chemical shift difference ($\Delta\delta$) between the two multiplets decreases ($Ti > Zr \approx Hf$) with an increase in the atomic radius of the metal ($Ti < Zr \approx Hf$). When the cycloalkylidene bridges were replaced by a 1,1-silacyclopentylidene bridge, the chemical shift differences between the two multiplets decrease clearly for the titanium complex **13** but increase slightly for the zirconium complex **14** (Table 1).

Abstract in Chinese:

摘要:合成了一系列亚烷基桥连环戊二烯基茂金属化合物 $(CH_2)_n C(C_5H_4)_2 MCl_2$ [$M = Ti$, $n = 4$ (**4**), **5** (**5**), **6** (**6**); $M = Zr$, $n = 4$ (**7**), **5** (**8**), **6** (**9**); $M = Hf$, $n = 4$ (**10**), **5** (**11**), **6** (**12**)]. 用甲基铝氧烷(MAO)作助催化剂研究了其催化乙烯聚合反应。其中亚烷基桥连环戊二烯基茂金属化合物的催化活性远高于相应的锆和铪类似物,且在较高温度显示其最高活性。为进行对比,合成了亚硅杂环戊二烯基桥连环戊二烯基茂金属化合物 $(CH_2)_4 Si(C_5H_4)_2 MCl_2$ ($M = Ti$, Zr)和亚异丙基桥连环戊二烯基茂金属化合物 $Me_2C(C_5H_4)_2 MCl_2$ ($M = Ti$, Zr)并用于催化乙烯聚合。在这两种催化剂中,钛化合物的催化活性都远高于相应的锆类似物,尤其是在较低温度下。用X-射线衍射分析测定了化合物 **4**–**9** 的晶体结构。对催化剂结构与催化活性的关系,特别是桥链的影响进行了讨论。

Table 1. 1H NMR spectra data for complexes **4**–**14**.

Complex	$\delta(C_5H_4)$	$(\Delta\delta)$
4	6.95 (m, 4H), 5.62 (m, 4H)	1.33
5	6.96 (m, 4H), 5.63 (m, 4H)	1.33
6	6.95 (m, 4H), 5.62 (m, 4H)	1.33
7	6.64 (m, 4H), 5.71 (m, 4H)	0.93
8	6.56 (m, 4H), 5.69 (m, 4H)	0.87
9	6.65 (m, 4H), 5.76 (m, 4H)	0.89
10	6.55 (m, 4H), 5.64 (m, 4H)	0.91
11	6.65 (m, 4H), 5.76 (m, 4H)	0.89
12	6.56 (m, 4H), 5.69 (m, 4H)	0.87
13	7.10 (m, 4H), 5.96 (m, 4H)	1.14
14	6.96 (m, 4H), 5.98 (m, 4H)	0.98

Molecular structures: The molecular structures of complexes **4–9** have been determined by X-ray diffraction and they are depicted in Figures 1–6. Tables 2 and 3 present some selected bond lengths and bond angles, respectively.

The cycloalkylidene-bridged metallocene complexes have similar structures to the isopropylene-bridged metallocene

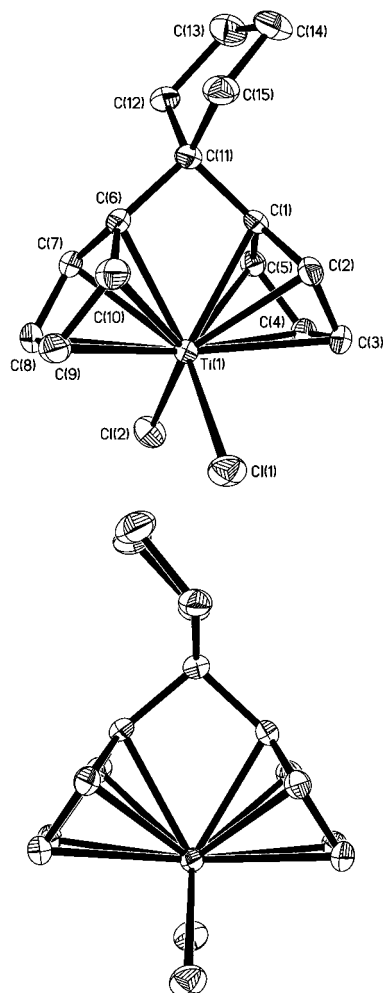


Figure 1. Molecular structure of complex **4** (ORTEP diagram; thermal ellipsoids are shown at the 30 % level).

complexes $[\text{Me}_2\text{C}(\text{C}_5\text{H}_4)_2\text{MCl}_2]$,^[11] but with significant distortions of the geometry due to the introduction of the unsymmetrical cycloalkylidene bridge. In these structures, the bridging cyclopentyl moiety adopts a normal envelope conformation, the bridging cyclohexyl moiety a normal chair conformation, and the bridging cycloheptyl moiety an approximate chair conformation. The C(Cp)–C(bridge)–C(Cp) angles are 96.9(2), 96.6(2), 96.3(2), 99.8(5), 99.7(5), and 99.1(2)° for complexes **4–9**, respectively: that is, they are smaller than those expected for tetrahedral carbon by about 13° for the titanocenes **4–6** and 10° for the zirconocenes **7–9**. The Cen–M–Cen angles (Cen denotes the centroid of cyclopentadienyl ring) are 121.1–121.4° for the titanocenes **4–6**

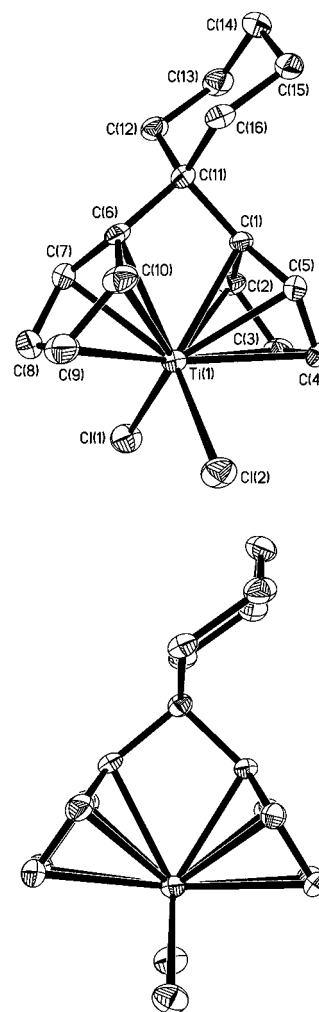


Figure 2. Molecular structure of complex **5** (ORTEP diagram; thermal ellipsoids are shown at the 30 % level).

and 116.3–116.6° for the zirconocenes **7–9**, about 10° and 13° smaller than those of $[\text{Cp}_2\text{TiCl}_2]$ (131.0°)^[12] and $[\text{Cp}_2\text{ZrCl}_2]$ (129.3°),^[13] indicating an opening of the wedge formed by the two cyclopentadienyl ligands. This is accompanied by the larger Cl–M–Cl angles of 97.0–97.5° for the titanocenes **4–6** and 99.5–100.5° for the zirconocenes **7–9** compared to the corresponding values of 94.53(6)° in $[\text{Cp}_2\text{TiCl}_2]$ and 97.1(2)° in $[\text{Cp}_2\text{ZrCl}_2]$. The dihedral angles $\angle \text{Cp}–\text{Cp}$ are 65.6, 65.7, 65.5, 71.2, 69.9, and 69.5° for complexes **4–9**, respectively, so they are significantly larger than those in $[\text{Cp}_2\text{TiCl}_2]$ (58.5°) and in $[\text{Cp}_2\text{ZrCl}_2]$ (53.5°), but slightly smaller than those in $[\text{Me}_2\text{C}(\text{C}_5\text{H}_4)_2\text{MCl}_2]$ (66.9° for M = Ti, 71.4° for M = Zr). The average C–C bond lengths in cyclopentadienyl rings are 1.407 Å for the titanocenes **4–6**, slightly shorter than that in $[\text{Me}_2\text{C}(\text{C}_5\text{H}_4)_2\text{TiCl}_2]$ (1.414 Å), but much longer than that in $[\text{Cp}_2\text{TiCl}_2]$ (1.370 Å). The average C–C bond lengths of cyclopentadienyl rings are 1.423, 1.411, and 1.408 Å for the zirconocenes **7–9**, respectively, comparable with that in $[\text{Me}_2\text{C}(\text{C}_5\text{H}_4)_2\text{ZrCl}_2]$ (1.411 Å), but much longer than that in $[\text{Cp}_2\text{ZrCl}_2]$ (1.395 Å). Similarly to

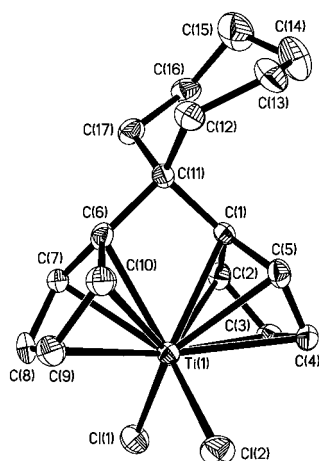


Figure 3. Molecular structure of complex **6** (ORTEP diagram; thermal ellipsoids are shown at the 30 % level).

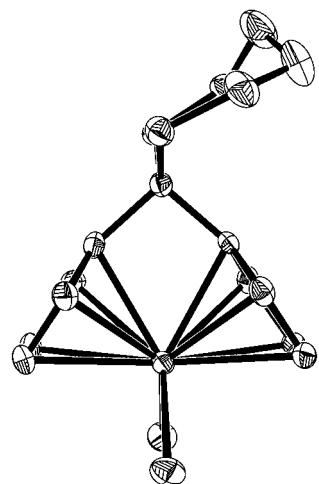
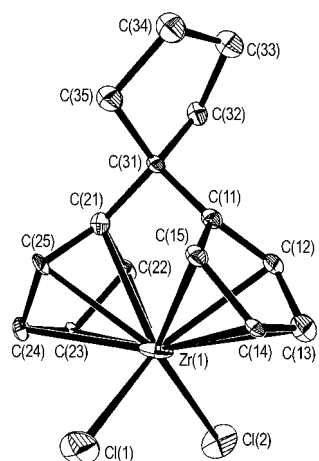


Figure 4. Molecular structure of complex **7** (ORTEP diagram; thermal ellipsoids are shown at the 30 % level).



the 1-methyl-4,4-piperidynylene-bridged zirconocene dichlorides and cyclohexylidene-bridged cyclopentadienyl and indenyl titanocene $[(\text{CH}_2)_5\text{C}(\text{C}_5\text{H}_4)(\text{C}_9\text{H}_6)\text{TiCl}_2]$,^[14] the dis-

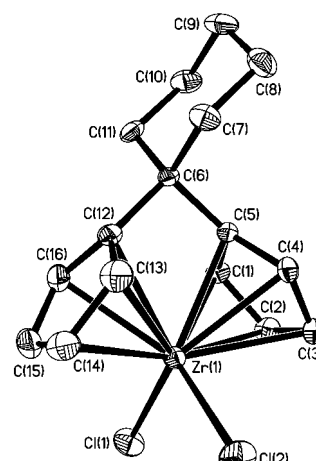


Figure 5. Molecular structure of complex **8** (ORTEP diagram; thermal ellipsoids are shown at the 30 % level).

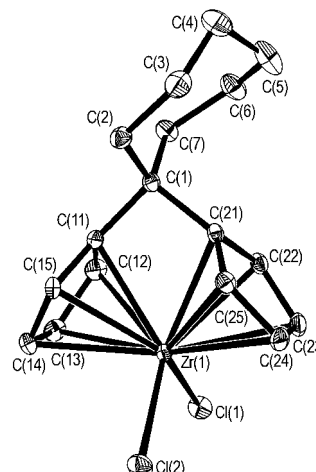


Figure 6. Molecular structure of complex **9** (ORTEP diagram; thermal ellipsoids are shown at the 30 % level).

ces from the metal to the ring carbon atoms are not equal. The M–C distances at the opposite side of the complexes are longer than those at the bridge position by 0.09, 0.10, 0.09, 0.14, 0.10, and 0.08 Å for complexes **4–9**, on average.

The C–C bond lengths of the bridging cyclopentylidene and cyclohexylidene rings are between 1.51 and 1.55 Å, the normal range for C–C single bond lengths. However, there are some C–C bonds at the ends of the bridging cycloheptylidene rings in complexes **6** and **9** (C(14)–C(15) 1.465(7), C(13)–C(14) 1.497(6), C(12)–C(13) 1.501(6) Å for **6**, and C(5)–C(6) 1.474(10), C(4)–C(5) 1.498(11) Å for **9**) that are significantly shorter than the others (1.529–1.552 Å for **6** and 1.513–1.544 Å for **9**), indicating that there are stronger nonbonding interactions between the bulky bridging cycloheptylidene ring and cyclopentadienyl groups. The nonbonding interactions may compress two cyclopentadienyl rings to form a slightly smaller $\angle\text{Cp-Cp}$ angle and strengthen the M–Cp bonds. The average M–C(Cp) bond lengths are

Table 2. Selected bond lengths [Å] and angles [°] for (CH₂)_nC(C₅H₄)₂TiCl₂ (*n* = 4, 5, 6).

	<i>n</i> = 4 (4)	<i>n</i> = 5 (5)	<i>n</i> = 6 (6)
Ti–Cl(1)	2.3464(11)	2.3469(13)	2.3415(15)
Ti–Cl(2)	2.3380(11)	2.3439(12)	2.3538(15)
Ti–C(1)	2.337(3)	2.336(3)	2.333(4)
Ti–C(2)	2.350(3)	2.353(3)	2.326(4)
Ti–C(3)	2.442(3)	2.454(3)	2.429(4)
Ti–C(4)	2.439(3)	2.432(3)	2.430(4)
Ti–C(5)	2.345(3)	2.336(3)	2.345(4)
Ti–C(6)	2.329(3)	2.334(3)	2.327(4)
Ti–C(7)	2.334(3)	2.342(3)	2.331(4)
Ti–C(8)	2.412(3)	2.411(4)	2.413(4)
Ti–C(9)	2.409(3)	2.409(4)	2.412(4)
Ti–C(10)	2.338(3)	2.333(3)	2.325(4)
C(1)–C(2)	1.416(4)	1.407(4)	1.423(6)
C(2)–C(3)	1.412(4)	1.418(4)	1.400(5)
C(3)–C(4)	1.379(4)	1.381(4)	1.377(5)
C(4)–C(5)	1.416(4)	1.409(4)	1.425(6)
C(1)–C(5)	1.414(4)	1.421(4)	1.412(5)
C(6)–C(7)	1.408(4)	1.409(4)	1.423(6)
C(7)–C(8)	1.407(4)	1.420(5)	1.409(6)
C(8)–C(9)	1.387(5)	1.378(5)	1.389(6)
C(9)–C(10)	1.410(5)	1.400(5)	1.391(6)
C(6)–C(10)	1.420(4)	1.421(4)	1.414(5)
C(1)–C(11)	1.534(4)	1.534(4)	1.517(5)
C(6)–C(11)	1.520(4)	1.525(4)	1.530(5)
C(11)–C(12)	1.534(4)	1.542(4)	1.552(5)
C(11)–C(11+ <i>n</i>)	1.532(4)	1.529(4)	1.550(5)
C(12)–C(13)	1.519(4)	1.518(5)	1.501(6)
C(13)–C(14)	1.525(5)	1.520(5)	1.497(6)
C(14)–C(15)	1.527(4)	1.522(5)	1.465(7)
C(15)–C(16)	–	1.517(5)	1.540(7)
C(16)–C(17)	–	–	1.529(5)
M–Cen ^[a]	2.061	2.061	2.049
	2.040	2.042	2.037
C(1)–C(6)	2.286	2.284	2.275
Cl–Ti–Cl	96.98(3)	97.41(4)	97.54(5)
Cen–Ti–Cen	121.1	121.1	121.4
C(1)–C(11)–C(6)	96.9(2)	96.6(2)	96.6(3)
C(12)–C(11)–C(11+ <i>n</i>)	102.2(2)	108.6(2)	109.9(3)
C(1)–C(11)–(12)	113.5(2)	112.2(2)	114.1(3)
C(1)–C(11)–C(11+ <i>n</i>)	112.6(2)	112.9(2)	113.6(3)
C(6)–C(11)–(12)	115.5(2)	113.0(2)	111.5(3)
C(6)–C(11)–C(11+ <i>n</i>)	116.7(2)	113.3(3)	110.5(3)
✕ Cp–Cp ^[b]	65.6	65.7	65.6

[a] Cen denotes the centroid of the cyclopentadiene ring. [b] ✕ Cp–Cp means the dihedral angles between two Cp planes.

2.383, 2.374, 2.368, 2.507, 2.499, and 2.485 Å for complexes **4–9**, respectively, decreasing with an increase in the cycloalkylidene ring size. In comparison with the corresponding [Me₂C(C₅H₄)₂MCl₂] (av Ti–C(Cp) 2.381 Å; Zr–C(Cp) 2.498 Å) and [Me₂Si(C₅H₄)₂MCl₂] (av Ti–C(Cp) 2.394 Å; Zr–C(Cp) 2.500 Å),^[15] introduction of cycloalkylidene bridges, especially introduction of a bulky cycloheptylidene bridge, significantly strengthens the M–Cp bonds, due to the larger nonbonding interactions between the cycloheptylidene ring and cyclopentadienyl groups. The average M–Cen

Table 3. Selected bond lengths [Å] and angles [°] for (CH₂)_nC(C₅H₄)₂ZrCl₂ (*n* = 4, 5, 6).

	<i>n</i> = 4 (7)	<i>n</i> = 5 (8)	<i>n</i> = 6 (9)
Zr–Cl(1)	2.436(2)	2.442(2)	2.441(1)
Zr–Cl(2)	2.429(2)	2.447(3)	2.433(1)
Zr–C(Cp)	2.442–2.589	2.455–2.572	2.446–2.539
C(Cp)–C(Cp)	1.36–1.46	1.397–1.427	1.369–1.422
C(bridge)–C(Cp)	1.50(2)	1.533(9)	1.537 (4)
	1.55(2)	1.540(9)	1.530 (5)
C–C(cycloalkylidene)	1.51–1.55	1.515–1.550	1.474–1.544
M–Cen	2.197	2.199	2.171
	2.185	2.184	2.184
C–C(bridgehead)	2.333	2.349	2.334
Cl–Zr–Cl	100.51(7)	99.48(7)	100.0(1)
Cen–Zr–Cen	116.6	116.4	116.3
C(Cp)–C(bridge)–C(Cp)	99.8(5)	99.7(5)	99.1(2)
✕ Cp–Cp	71.2	69.9	69.5

distances are 2.051, 2.052, 2.043, 2.191, 2.192, and 2.178 Å for complexes **4–9**, respectively, which are consistent with the trend in M–C(Cp) bond lengths.

The other distinct structural alteration introduced by cycloalkylidene bridges is the nonequivalent coordination of two cyclopentadienyl groups. The differences in M–Cl bonds are 0.008, 0.003, 0.012, 0.008, 0.005, and 0.008 Å for complexes **4–9**, respectively. The differences in average M–C(Cp) bond lengths for two cyclopentadienyl rings are 0.037, 0.016, 0.011, 0.010, 0.017, and 0.012 Å for complexes **4–9**, respectively, decreasing with an increase in the cycloalkylidene ring size for titanocenes. This indicates that the introduction of cycloalkylidene bridges causes more significant effects on the structures of titanocenes than on those of zirconocenes, because the atomic radius of titanium is smaller than that of zirconium. The differences in average M–Cen distances for the two cyclopentadienyl rings are 0.021, 0.019, 0.012, 0.012, 0.015, and 0.013 Å for **4–9**, respectively, consistent with the trend in M–C(Cp) distances.

Ethylene polymerization: The results of ethylene polymerization obtained with complexes **4–16** activated by MAO (Tables 4–6) show that the cycloalkylidene-bridged cyclo-

Table 4. Ethylene polymerization with **4–12**/MAO catalyst systems. Polymerization conditions: Al/M = 2500:1, temperature = 60 °C, monomer pressure = 1 atm, in 100 mL toluene. For **4–6**: catalyst concentration = 3.0 × 10^{−6} M, time = 15 min; for **7–12**: catalyst concentration = 1.0 × 10^{−5} M, time = 30 min.

Catalyst	4	5	6	7	8	9	10	11	12
A ^[a]	27.0	37.4	19.5	0.46	1.00	1.40	0.03	0.02	0.30

[a] A: Activity in (kg PE)(mmol M)^{−1} h^{−1}.

pentadienyl Group 4 metallocene complexes **4–12** exhibit diverse activities for ethylene polymerization (Table 4). Similarly to many analogues,^[2,3] the zirconocenes show higher activities than the hafnocenes. However, the activities (up to 3.74 × 10⁷ (g PE)(mmol Ti)^{−1} h^{−1}) of the cycloalkylidene-bridged cyclopentadienyl titanocenes **4–6** are an order of

magnitude higher than those of the corresponding zirconocenes and hafnocenes.

From Table 5, the temperature at which the activity of the titanocenes is highest increases with an increase in the cycloalkylidene bridge size (**4**, 60 °C; **5**, 60 °C; **6**, 70 °C), indicating

Table 5. Ethylene polymerization with cycloalkylidene-bridged titanocenes **4–6**/MAO catalyst systems at various temperatures. Polymerization conditions: Al/M = 2500:1, monomer pressure = 1 atm, in 100 mL toluene, catalyst concentration = 3.0×10^{-6} M, time = 15 min.

Catalyst	T_p [°C] ^[a]	Yield [g]	Activity [(kg PE) (mmol Ti) ⁻¹ h ⁻¹]	$10^4 \times M_w$ [g mol ⁻¹] ^[b]	M_w/M_n
4	30	0.65	8.70	97.4	2.71
	40	0.68	9.10	64.6	2.33
	50	0.93	12.3	64.2	2.35
	60	2.02	27.0	37.1	1.98
	70	1.12	15.0	32.4	2.07
5	30	0.87	11.6	67.0	4.03
	40	0.37	4.95	40.5	4.97
	50	0.34	4.48	32.6	3.90
	60	2.80	37.4	29.6	2.29
	70	0.90	11.9	23.5	2.17
6	30	0.72	9.62	85.8	2.74
	40	0.72	9.65	45.5	2.77
	50	1.42	18.9	35.0	3.03
	60	1.46	19.5	27.8	2.26
	70	1.75	23.3	21.7	2.03

[a] Polymerization temperature. [b] Determined by GPC.

that the thermal stability of titanocene catalysts increases with increasing length of the cycloalkylidene bridge. The weight-average molecular weights are close to 10^6 at a low temperature (30 °C) and decrease with increasing temperature. The GPC curves of the polyethylene obtained appeared unimodal, and the molecular weight distribution (MWD; M_w/M_n) values are close to 2 (2.07, 2.17, and 2.03 for **4**, **5**, and **6**) at a higher temperature (70 °C), indicating that they belong to single-site catalyst systems.

The silacyclopentylidene- and isopropylene-bridged metallocene complexes **13–16** gave similar results (Table 6). The titanocenes **13** and **15** showed much higher activities than the corresponding zirconocenes, especially at the lower temperature. The activity of the silacyclopentylidene-bridged titanocene **13** decreased sharply with increasing temperature, indicating its poor thermal stability. The molecular weights of the polyethylene produced by the titanocenes **13** and **15** were also much higher than that by the zirconocenes **14** and **16**. The MWDs were broader, especially for the isopropylene-bridged zirconocene **16**, which reached 14–17. The GPC curves of the polyethylene obtained appeared generally bimodal or trimodal, indicating decomposition of the catalysts during polymerization.

Structure–activity relationships: It is now generally recognized that zirconocene catalysts are much more active than titanocenes and hafnocenes in olefin polymerization.^[2,3] The generally low activity of Ti can be attributed to its tendency to be reduced or to exhibit poor thermal stability,^[2c,16] while the low activity of Hf complexes has been attributed to the

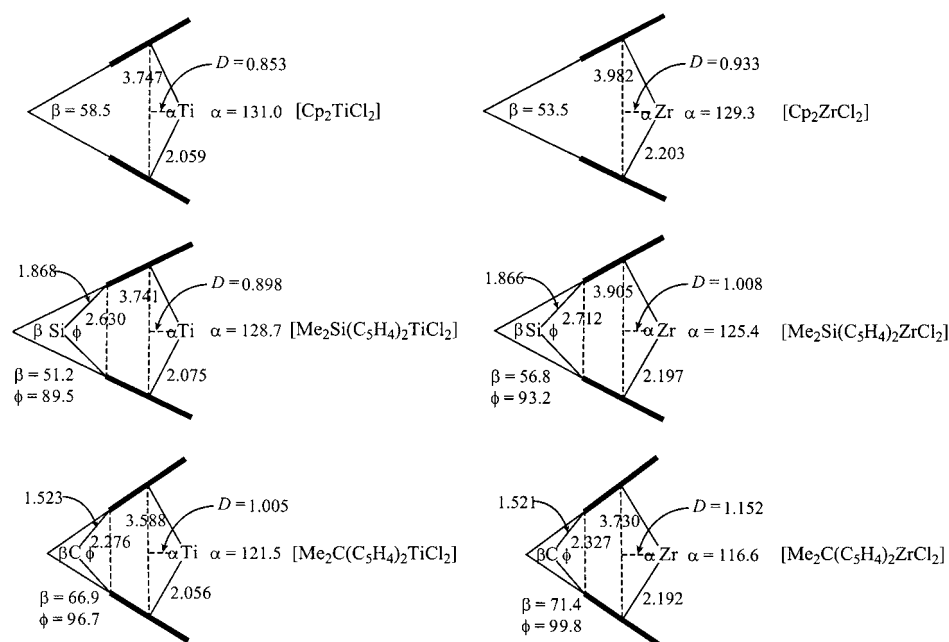
Table 6. Ethylene polymerization with **13–16**/MAO catalyst systems. Polymerization conditions: Al/M = 2500, temperature = 60 °C, monomer pressure = 1 atm, in 100 mL toluene. For **13** and **15**: catalyst concentration = 3.0×10^{-6} M, time = 15 min; for **14** and **16**: catalyst concentration = 1.0×10^{-5} M, time = 30 min.

Catalyst	T_p [°C] ^[a]	Yield [g]	Activity [(kg PE) (mmol Ti) ⁻¹ h ⁻¹]	$10^4 \times M_w$ [g mol ⁻¹] ^[b]	M_w/M_n
13	30	1.040	13.9	70.1	2.24
	40	0.975	13.0	54.2	2.16
	50	0.809	10.8	29.4	2.63
	60	0.309	4.12	19.6	2.56
	70	0.037	0.49		
14	30	0.298	0.60	22.9	5.18
	40	0.493	0.99	13.8	4.19
	50	0.454	0.91	6.41	3.56
	60	0.381	0.76	2.59	2.75
	70				
15	30	1.083	14.4	74.0	6.68
	40	1.350	18.0	57.5	2.55
	50	1.944	25.9	47.8	2.75
	60	0.751	10.0	36.6	4.26
	70	0.342	4.56	23.3	5.09
16	30	0.083	0.166	25.4	17.09
	40	0.065	0.130	16.1	15.93
	50	0.054	0.108	10.5	14.83
	60	0.038	0.076		

[a] Polymerization temperature. [b] Determined by GPC.

greater strength of the Hf–C bond compared to the Zr–C bond^[2c] or to kinetic reasons (slow olefin coordination and insertion step).^[2b] However, at a low temperature the titanocenes usually show higher activities than the zirconocenes for polymerization of ethylene and even of propylene.^[17,18] A stereorigid bridged metallocene cation usually has closely equivalent metal–centroid bond lengths and angles, as does its neutral precursor^[19], and thus the latter structure may be relied on as a model for the former, and for interpretation of the polymerization results. To explain our polymerization results and find the structure–activity relationships, especially the effects of the bridges of ansa-metallocene complexes, the relevant geometrical parameters of unbridged metallocene complexes [Cp₂MCl₂], dimethylsilylene-bridged metallocene complexes [(Me₂Si)(C₅H₄)₂MCl₂], and isopropylene-bridged metallocene complexes [(Me₂C)(C₅H₄)₂MCl₂] (M = Ti, Zr) are compared in Scheme 3 and Table 7. The incorporation of a bridging unit in the metallocene dichloride has geometrical consequences that depend on the number and nature of atoms in the bridge. For the purpose of discussion, only systems that contained a single-atom bridging unit and no other ring substituents were chosen for comparison.

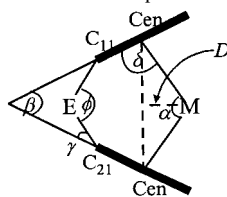
For the zirconocenes, after introduction of a bridge the Zr–Cen distances decrease slightly with the bridge shortening (2.203, 2.197, and 2.192 Å for [Cp₂ZrCl₂], [Me₂Si(C₅H₄)₂ZrCl₂], and [Me₂C(C₅H₄)₂ZrCl₂], respectively), but the effects are small because of the larger atomic radius of zirconium. However, introduction of a bridge has significant effects on the other geometrical parameters of ansa-metallocene complexes. Introduction of a dimethylsilylene bridge shortens the Cen–Cen distance (3.905 Å versus 3.982 Å), increases the dihedral angle ∠Cp–Cp (56.8° versus 53.5°), de-



Scheme 3. Comparison of relevant geometrical parameters of selected metallocene complexes.

creases \angle Cen-Zr-Cen (125.4° versus 129.3°), and increases the D value (1.008 Å versus 0.933 Å; see Table 7). This increases the reaction space of the metal centers and the cata-

lytic activity for ethylene polymerization. Introduction of a short isopropylene bridge makes the Cen-Cen distance much shorter (3.730 Å), increases the dihedral angle \angle Cp-Cp further to 71.4°, decreases \angle Cen-Zr-Cen further to 116.6°, and increases the D value to 1.152 Å. The metal atom moves out much further than in the unbridged and dimethylsilylene-bridged analogues. Although the reaction space of the metal center is further increased, this makes the stability of the isopropylene-bridged zirconocene decrease significantly. This has been further confirmed by the broader MWD values (14–17) and the bimodal or trimodal GPC curves of the polyethylene produced by the isopropylene-

Table 7. Relevant geometrical parameters [° or Å] of selected metallocene complexes.^[a]

Complex	φ [°]	C ₁₁ -C ₂₁ [Å]	E-C [Å]	Cen-Cen [°]	D [Å]	α [°]	χ [°]	δ [°]	β [°]	M-Cen [Å]	Ref.
[Cp ₂ TiCl ₂]				3.747	0.853	131.0		85.3	58.5	2.059	12
[Me ₂ Si(C ₅ H ₄) ₂ TiCl ₂]	89.5(1)	2.630	1.868(2)	3.741	0.898	128.7	19.2	90.1	51.2	2.075	14
[Me ₂ C(C ₅ H ₄) ₂ TiCl ₂]	96.7(1)	2.276	1.523(2)	3.588	1.005	121.5	14.9	85.8	66.9	2.056	11
[(CH ₂) ₄ C(C ₅ H ₄) ₂ TiCl ₂]	96.9(2)	2.286	1.534(4)	3.571	1.008	121.1	15.1	86.1	65.6	2.061	this work
			1.520(4)				15.0	86.9		2.040	
[(CH ₂) ₅ C(C ₅ H ₄) ₂ TiCl ₂]	96.6(2)	2.284	1.534(4)	3.573	1.009	121.1	14.5	85.9	65.7	2.061	this work
			1.525(4)				15.2	87.0		2.042	
[(CH ₂) ₆ C(C ₅ H ₄) ₂ TiCl ₂]	96.6(3)	2.275	1.517(5)	3.563	1.000	121.4	14.6	86.2	65.6	2.049	this work
			1.530(5)				15.1	86.8		2.037	
[(CH ₂) ₄ Si(C ₅ H ₄) ₂ TiCl ₂] ^[b]	90.7		1.863	3.736	0.889	129.1	18.6	87.9	55.7	2.069	18
[Cp ₂ ZrCl ₂]				3.982	0.933	129.3		88.8	53.5	2.203	13
[Me ₂ Si(C ₅ H ₄) ₂ ZrCl ₂]	93.2(2)	2.712	1.866(4)	3.905	1.008	125.4	18.2	88.9	56.8	2.197	14
[Me ₂ C(C ₅ H ₄) ₂ ZrCl ₂]	99.8(2)	2.327	1.521(2)	3.730	1.152	116.6	14.2	86.0	71.4	2.192	11
[(CH ₂) ₄ C(C ₅ H ₄) ₂ ZrCl ₂]	99.8(5)	2.333	1.50(2)	3.728	1.151	116.6	13.5	85.2	71.2	2.197	this work
			1.55(2)				14.2	87.4		2.185	
[(CH ₂) ₅ C(C ₅ H ₄) ₂ ZrCl ₂]	99.7(5)	2.349	1.533(9)	3.725	1.155	116.4	14.6	86.5	69.9	2.199	this work
			1.540(9)				14.5	87.1		2.184	
[(CH ₂) ₆ C(C ₅ H ₄) ₂ ZrCl ₂]	99.1(2)	2.334	1.537(4)	3.699	1.149	116.3	14.2	87.4	69.5	2.171	this work
			1.530(5)				14.3	86.9		2.184	
[(CH ₂) ₄ Si(C ₅ H ₄) ₂ ZrCl ₂]	94.3(3)		1.878(7)	3.915	1.006	125.6	18.5	87.7	59.1	2.201	18
			1.866(8)								

[a] In the schematic representation of an ansa-metallocene molecule above,^[20] φ is the angle C(bridgehead)-E-C(bridgehead); δ is the angle between the M-Cen vector and the Cp plane; χ is the angle between the E-C(bridgehead) vector and the Cp plane; β is the dihedral angle between the two Cp planes; α is the angle Cen-M-Cen. [b] The average values are given, due to the existence of two independent molecules in the unit.

the catalytic activities of other single carbon-atom bridged zirconocenes are lower than those of single silicon-atom bridged analogues for ethylene polymerization.^[21]

For the titanocenes, after introduction of a dimethylsilylene bridge the Cen–Cen distance is nearly unchanged (3.741 Å versus 3.747 Å), the \angle Cen–Ti–Cen angle decreases slightly (128.7° versus 131.0°), and the *D* value increases slightly (0.898 Å versus 0.853 Å), but the dihedral angle \angle Cp–Cp decreases from 58.5° to 51.2°. The Ti–Cen distances increase more evidently than the unbridged titanocene [Cp₂TiCl₂] (2.075 Å versus 2.059 Å), because the dimensions of the large silicon-atom bridge do not match the coordination requirement of the small titanium atom. This means that not only is the reaction space of the metal center not increased, but the stability of the titanocene is also decreased after being bridged with the dimethylsilylene group. Also, the dimethylsilylene-bridged titanocenes show lower activity for ethylene polymerization.^[2,3,8]

After introduction of an isopropylene bridge, the Ti–Cen distances are nearly equal to those in the unbridged titanocene [Cp₂TiCl₂] (2.056 Å versus 2.059 Å), but much shorter than those of the dimethylsilylene-bridged titanocene. This indicates that the small bridging carbon atom and the small titanium atom can be matched. Introduction of an isopropylene bridge shortens the Cen–Cen distance (3.588 Å), increases the dihedral angle \angle Cp–Cp to 66.9°, decreases \angle Cen–Zr–Cen to 121.5°, and increases the *D* value to 1.005 Å. The reaction space of the metal centers is increased significantly, but the stability of the isopropylene-bridged titanocene hardly decreases, due to the similar Ti–Cen distances (in comparison with [Cp₂TiCl₂]), smaller differences in the dihedral angles and \angle Cen–M–Cen ($\Delta\beta$ = 8.4°, $\Delta\alpha$ = 9.5°, in comparison with [Cp₂TiCl₂]) than in the corresponding zirconocene analogues ($\Delta\beta$ = 17.9°, $\Delta\alpha$ = 12.7°, in comparison with [Cp₂ZrCl₂]). So the isopropylene-bridged titanocene **15** shows higher activity for ethylene polymerization than even the corresponding zirconocene analogue **16**.

Ethylidene(1-tetramethylcyclopentadienyl)(1-indenyl) dichlorozirconium/MAO has an ethylene polymerization activity of about 10⁴ (g PE)(mol Zr)^{−1}[C₂H₄]^{−1}h^{−1}, which is four orders of magnitude lower than that of [Cp₂ZrCl₂]/MAO^[22]. The polyethylene produced has bimodal distributions, indicating two or more active species. The activity for propylene polymerization is even lower (<10⁴). In contrast, the titanium analogue does polymerize propylene to high molecular weight polymer. Analysis of the structure–catalysis relationships further supported our views.

The cycloalkylidene-bridged titanocenes have similar geometrical parameters to isopropylene-bridged titanocene **15**. However, the dihedral angles \angle Cp–Cp are slightly decreased (65.6, 65.7, and 65.6° for **4–6**, respectively, versus 66.9° for **15**), but are still much larger than that of [Cp₂TiCl₂]. The Cen–Cen distances (3.571, 3.573, and 3.563 Å for **4–6** versus 3.588 Å for **15**) and the average M–Cen distances (2.051, 2.052, and 2.043 Å for **4–6**, versus 2.056 Å for **15**) decrease with an increase in the bridging cycloalkylidene ring size, due to the nonbonded interactions

between the cycloalkylidene bridges and cyclopentadienyl groups. This greatly improves the stabilities of the cycloalkylidene-bridged titanocenes while retaining the large reaction space of the metal center. This is consistent with the polymerization results. In particular, the cycloheptylidene-bridged titanocene **6** shows the highest activity at a higher temperature (70°C).

In an attempt to explain the polymerization results for silacyclopentylidene-bridged metallocene complexes, Kim et al.^[18] recently reported the syntheses and structures of a series of 1,1-silacycloalkylidene-bridged metallocene complexes and found the 1,1-silacycloalkylidene-bridged titanocenes also exhibited remarkable activities in comparison with the corresponding zirconocenes. The activities are also higher than the acyclic dimethylsilylene-bridged analogue, [Me₂Si(C₅H₄)₂TiCl₂]. Their explanation was that the presence of silacycloalkylidene bridges increases the stabilities of the titanocene complexes. This is consistent with our viewpoint. By comparing the structural parameters, it can be found that replacement of the dimethylsilylene bridge with a silacyclopentylidene bridge causes different effects on the titanocenes and zirconocenes. The dihedral angle increases much more for the titanocene **13** (55.7° versus 51.2°) than for the zirconocene **14** (59.1° versus 56.8°), indicating enlargement of the reaction space of the metal center, especially for the titanocene. For the 1,1-silacyclopentylidene-bridged titanocene, \angle Cen–Ti–Cen also increases slightly (129.1° versus 128.7°), while the Ti–Cen distances (2.069 versus 2.075 Å), the *D* value (0.889 versus 0.898 Å), and the Cen–Cen distance (3.736 versus 3.741 Å) decrease slightly. For the 1,1-silacyclopentylidene-bridged zirconocene, however, \angle Cen–Zr–Cen (125.6° versus 125.4°) and the *D* value (1.006 versus 1.008 Å) are nearly unchanged, whereas the Zr–Cen distances (2.201 versus 2.197 Å) and the Cen–Cen distance (3.915 versus 3.905 Å) decrease slightly. This indicates that the presence of silacycloalkylidene bridges brings the two Cp ligands closer together and increases the stabilities of the titanocene complexes but has little effect on the zirconocene complexes. Therefore the silacyclopentylidene-bridged titanocene **13** shows higher activity at low temperatures than the corresponding zirconocene analogue **14**. However, because the dimensions of the large silicon-atom bridge and the small titanium atom are unmatched, the titanocene **13** still has a low thermal stability and the activity for ethylene polymerization decreases sharply with increasing temperature. At a higher temperature (70°C) the activity is nearly comparable with that of the corresponding zirconocene analogue **14**.

Conclusion

A series of cycloalkylidene-bridged cyclopentadienyl metallocene complexes, [(CH₂)_{*n*}C(C₅H₄)₂MCl₂] (M = Ti, *n* = 4 (**4**), 5 (**5**), 6 (**6**); M = Zr, *n* = 4 (**7**), 5 (**8**), 6 (**9**); M = Hf, *n* = 4 (**10**), 5 (**11**), 6 (**12**)), have been synthesized and applied to ethylene polymerization. The cycloalkylidene-bridged ti-

tanocene catalysts exhibit much higher activities than the corresponding zirconocene and hafnocene analogues, and have the highest activities at higher temperatures. In comparison, the 1,1-silacyclopentylidene-bridged metallocene complexes $[(CH_2)_4Si(C_5H_4)_2MCl_2]$ ($M = Ti$ (**13**), Zr (**14**)), and isopropylene-bridged metallocene complexes $[Me_2C(C_3H_4)_2MCl_2]$ ($M = Ti$ (**15**), Zr (**16**)) have also been synthesized and applied to ethylene polymerization. In both cases, the titanocene complexes exhibit much higher activities than the corresponding zirconocene analogues, especially at the lower temperature. The structure–activity relationships study shows that the dimensions of the small carbon-atom bridge match up well to the coordination requirement of the small titanium atom, while the dimensions of the large silicon-atom bridge match up well to the coordination requirement of the large zirconium atom. Both of these bridged complexes achieve the largest reaction space of the metal center while retaining the stability of the metallocene complexes, and show higher activities than the unbridged and other bridged metallocene complexes. The introduction of a cycloalkylidene or 1,1-silacyclopentylidene bridge, especially the bulky cycloheptylidene bridge, may increase the stability of the ansa-titanocenes and increase their activity for ethylene polymerization.

Experimental Section

General: All operations were carried out under an argon atmosphere using standard Schlenk techniques. Toluene, hexane, and tetrahydrofuran (THF) were purified by refluxing over a sodium/ $(C_6H_5)_2CO$ system under argon. Dichloromethane was distilled from P_2O_5 . Polymerization grade ethylene (Yanshan Petrochem. Co., China) was used without further purification. 1H NMR spectra were recorded on a Bruker AC-P200 spectrometer. Mass spectra were measured on a VG 7070E HF instrument (EI, 70 eV; only important mass peaks are reported). Elemental analyses were performed on a CHN Corder MF-3 analyzer. $(CH_2)_4C(C_5H_5)_2$ (**1**),^[10] $(CH_2)_3C(C_5H_5)_2$ (**2**),^[10] $[(Me_2C)(C_5H_4)_2TiCl_2]$ (**15**),^[11] and $[(Me_2C)(C_5H_4)_2ZrCl_2]$ (**16**),^[11] $MCl_4 \cdot 2THF$ ($M = Ti, Zr, Hf$),^[23] and $(CH_2)_4SiCl_2$ ^[24] were prepared according to the literature methods. MAO was prepared from $Al_2(SO_4)_3 \cdot 18H_2O$ and trimethylaluminum in the usual manner.^[25]

Synthesis of $(CH_2)_6C(C_5H_5)_2$ (3**):** The freshly distilled cyclopentadiene (24 mL, 0.29 mol) was added to a suspension of NaOH powder (30 g) in THF (60 mL). The mixture was stirred for 2 h. Cycloheptanone (17.0 mL, 0.145 mol) in THF (10 mL) was added dropwise and the mixture was stirred for 2 h. The resulting mixture was hydrolyzed and the organic layer was separated, washed with water and dried (Na_2SO_4). The solvent was removed in vacuo and the residue was distilled (b.p. 106–114°C/0.1 mmHg) to give **3** as yellow oil. Yield: 16.0 g (49.1%); 1H NMR ($CDCl_3$, 25°C, TMS): $\delta = 1.54$ (brs, 8H; CH_2), 1.97–2.06 (m, 4H; CH_2), 2.75 (s), 2.95 (s) (total 4H; C_5H_5), 5.96–6.59 ppm (m, 6H; C_5H_5).

Synthesis of $[(CH_2)_4C(C_5H_4)_2TiCl_2]$ (4**):** A solution of $nBuLi$ (6.65 mL, 14.56 mmol) in hexane at 0°C was added to a solution of **1** (1.44 g, 7.28 mmol) in THF (20 mL). The mixture was stirred for 2 h at room temperature. Then a solution of $TiCl_4 \cdot 2THF$ (2.22 g, 7.28 mmol) in THF (15 mL) was added at 0°C. After the mixture had been stirred for 8 h at room temperature, the solvent was removed in vacuo. The residue was extracted with CH_2Cl_2 . Concentration and cooling of the CH_2Cl_2 solution afforded **4** as black crystals. Yield: 1.2 g (52.4%); m.p. 255°C (decomp); 1H NMR ($CDCl_3$, 25°C, TMS): $\delta = 6.95$ (m, 4H; C_5H_4), 5.57 (m, 4H; C_5H_4), 2.40–2.30 (m, 4H; CH_2), 2.00–1.90 ppm (m, 4H; CH_2); EI-MS

(70 eV): m/z (%): 314 (62) $[M^+]$, 278 (100) $[M^+ - HCl]$, 244 (22) $[M^+ - 2Cl]$, 242 (70) $[M^+ - 2HCl]$, 211 (15), 200 (18), 187 (11), 165 (15), 128 (19), 83 (29), 67 (28) $[C_5H_7^+]$; elemental analysis calcd (%) for $C_{15}H_{16}Cl_2Ti$ (315.06): C 57.18, H 5.12; found: C 57.10, H 5.36.

Synthesis of $[(CH_2)_5C(C_5H_4)_2TiCl_2]$ (5**):** Synthesis of **5** from **2**, $nBuLi$, and $TiCl_4 \cdot 2THF$ was similar to that described for **4**. Black crystals; yield: 1.0 g (37.9%); m.p. 260°C (decomp); 1H NMR ($CDCl_3$, 25°C, TMS): $\delta = 6.96$ (m, 4H; C_5H_4), 5.63 (m, 4H; C_5H_4), 2.30–2.20 (m, 4H; CH_2), 1.90–1.60 ppm (m, 6H; CH_2); EI-MS (70 eV): m/z (%): 328 (98) $[M^+]$, 292 (100) $[M^+ - HCl]$, 256 (80) $[M^+ - 2HCl]$, 224 (24), 211 (20), 200 (27), 187 (17), 165 (17), 128 (38), 118 (20, $[TiCl_2^+]$), 81 (77) $[C_6H_9^+]$; elemental analysis: calcd (%) for $C_{16}H_{18}Cl_2Ti$ (329.09): C 58.39, H 5.51; found: C 58.44, H 5.73.

Synthesis of $[(CH_2)_6C(C_5H_4)_2TiCl_2]$ (6**):** Synthesis of **6** from **3**, $nBuLi$, and $TiCl_4 \cdot 2THF$ was similar to that described for **4**. Black crystals; yield: 1.0 g (36.5%); m.p. 240°C (decomp); 1H NMR ($CDCl_3$, 25°C, TMS): $\delta = 6.95$ (m, 4H; C_5H_4), 5.62 (m, 4H; C_5H_4), 2.42–2.3 (m, 4H; CH_2), 1.92–1.67 ppm (m, 8H; CH_2); EI-MS (70 eV): m/z (%): 342 (47) $[M^+]$, 306 (71) $[M^+ - HCl]$, 270 (55) $[M^+ - 2HCl]$, 248 (22), 224 (27), 200 (29), 187 (21), 165 (23), 152 (33), 128 (41), 95 (78) $[C_7H_{11}^+]$, 83 (63), 67 (30) $[C_5H_7^+]$, 41 (100) $[C_3H_5^+]$; elemental analysis calcd (%) for $C_{17}H_{20}Cl_2Ti$ (343.12): C 59.51, H 5.87; found: C 59.42, H 5.63.

Synthesis of $[(CH_2)_4C(C_5H_4)_2ZrCl_2]$ (7**):** Synthesis of **7** from **1**, $nBuLi$, and $ZrCl_4 \cdot 2THF$ was similar to that described for **4**. Yellow crystals; yield: 0.53 g (18.5%); m.p. 270°C (decomp); 1H NMR ($CDCl_3$, 25°C, TMS): $\delta = 6.64$ (m, 4H; C_5H_4), 5.71 (m, 4H; C_5H_4), 2.40–2.30 (m, 4H; CH_2), 1.97–1.86 ppm (m, 4H; CH_2); EI-MS (70 eV): m/z (%): 356 (97) $[M^+]$, 321 (26) $[M^+ - Cl]$, 291 (40), 279 (47), 253 (42), 227 (42), 187 (19), 162 (33), 131 (100) $[C_5H_4C_3H_7^+]$, 83 (77); elemental analysis calcd (%) for $C_{15}H_{16}Cl_2Zr$ (358.42): C 50.26, H 4.50; found: C 50.29, H 4.51.

Synthesis of $(CH_2)_5C(C_5H_4)_2ZrCl_2$ (8**):** Synthesis of **8** from **2**, $nBuLi$, and $ZrCl_4 \cdot 2THF$ was similar to that described for **4**. Yellow crystals; yield: 1.5 g (50.5%); m.p. 272–274°C; 1H NMR ($CDCl_3$, 25°C, TMS): $\delta = 6.56$ (m, 4H; C_5H_4), 5.69 (m, 4H; C_5H_4), 2.33–2.22 (m, 4H; CH_2), 1.80–1.64 (m, 4H; CH_2), 1.63–1.52 ppm (m, 2H; CH_2); EI-MS (70 eV): m/z (%): 370 (100) $[M^+]$, 335 (31) $[M^+ - Cl]$, 298 (47) $[M^+ - 2HCl]$, 291 (35), 277 (59), 253 (39), 227 (43), 215 (21), 187 (20), 162 (41), 145 (19) $[C_5H_4C_6H_9^+]$, 77 (20); elemental analysis calcd (%) for $C_{16}H_{18}Cl_2Zr$ (372.45): C 51.60, H 4.87; found: C 51.52, H 4.92.

Synthesis of $[(CH_2)_6C(C_5H_4)_2ZrCl_2]$ (9**):** Synthesis of **9** from **3**, $nBuLi$, and $ZrCl_4 \cdot 2THF$ was similar to that described for **4**. Yellow crystals; yield: 0.50 g (24.4%); m.p. 241–242°C; 1H NMR ($CDCl_3$, 25°C, TMS): $\delta = 6.65$ (m, 4H; C_5H_4), 5.76 (m, 4H; C_5H_4), 2.45–2.35 (m, 4H; CH_2), 1.92–1.68 ppm (m, 8H; CH_2); EI-MS (70 eV): m/z (%): 384 (35) $[M^+]$, 349 (10) $[M^+ - Cl]$, 212 (12) $[M^+ - 2HCl]$, 291 (20), 277 (24), 253 (19), 227 (23), 162 (15), 83 (100), 41 (48); elemental analysis calcd (%) for $C_{17}H_{20}Cl_2Zr$ (386.48): C 52.83, H 5.22; found: C 52.85, H 5.23.

Synthesis of $[(CH_2)_4C(C_5H_4)_2HfCl_2]$ (10**):** Synthesis of **10** from **1**, $nBuLi$, and $HfCl_4 \cdot 2THF$ was similar to that described for **4**. White crystals; yield: 0.65 g (18.2%); m.p. 228°C (decomp); 1H NMR ($CDCl_3$, 25°C, TMS): $\delta = 6.55$ (m, 4H; C_5H_4), 5.64 (m, 4H; C_5H_4), 2.43–2.31 (m, 4H; CH_2), 1.99–1.87 ppm (m, 4H; CH_2); EI-MS (70 eV): m/z (%): 446 (69) $[M^+]$, 410 (11) $[M^+ - HCl]$, 381 (19), 367 (24), 353 (16), 315 (33), 250 (21), 165 (19), 155 (20), 131 (98) $[C_5H_4C_3H_7^+]$, 115 (39) $[C_5H_4C_4H_3^+]$, 67 (31) $[C_5H_7^+]$, 41 (100) $[C_3H_5^+]$; elemental analysis calcd (%) for $C_{15}H_{16}Cl_2Hf$ (445.69): C 40.42, H 3.62; found: C 40.44, H 3.91.

Synthesis of $[(CH_2)_5C(C_5H_4)_2HfCl_2]$ (11**):** Synthesis of **11** from **2**, $nBuLi$, and $HfCl_4 \cdot 2THF$ was similar to that described for **4**. White crystals; yield: 0.55 g (15.0%); m.p. 238°C (decomp); 1H NMR ($CDCl_3$, 25°C, TMS): $\delta = 6.65$ (m, 4H; C_5H_4), 5.76 (m, 4H; C_5H_4), 2.32–2.20 (m, 4H; CH_2), 1.82–1.66 (m, 4H; CH_2), 1.66–1.53 ppm (m, 2H; CH_2); EI-MS (70 eV): m/z (%): 460 (21) $[M^+]$, 424 (6) $[M^+ - HCl]$, 355 (9), 339 (9), 315 (13), 288 (10), 115 (17) $[C_5H_4C_4H_3^+]$, 77 (18), 67 (18) $[C_5H_7^+]$, 41 (100) $[C_3H_5^+]$; elemental analysis calcd (%) for $C_{16}H_{18}Cl_2Hf$ (459.71): C 41.80, H 3.95; found: C 41.89, H 4.13.

Synthesis of $[(CH_2)_6C(C_5H_4)_2HfCl_2]$ (12**):** Synthesis of **12** from **3**, $nBuLi$, and $HfCl_4 \cdot 2THF$ was similar to that described for **4**. Light green crystals;

yield: 0.91 g (24.0%); m.p. 229°C (dec.); ^1H NMR (CDCl_3 , 25°C, TMS): δ = 6.56 (m, 4H; C_5H_4), 5.69 (m, 4H; C_5H_4), 2.52–2.33 (m, 4H; CH_2), 1.90–1.62 ppm (m, 8H; CH_2); EI-MS (70 eV): m/z (%): 474 (9) [M^+], 438 (4) [$\text{M}^+ - \text{HCl}$], 391 (5), 381 (6), 367 (7), 354 (5), 341 (10), 115 (19) [$\text{C}_5\text{H}_4\text{C}_3\text{H}_3^+$], 91 (26), 77 (21), 55 (39), 41 (100) [C_3H_5^+]; elemental analysis calcd (%) for $\text{C}_{17}\text{H}_{20}\text{Cl}_2\text{Hf}$ (473.74): C 43.10, H 4.26; found: C 43.06, H 4.34.

Synthesis of $[(\text{CH}_2)_4\text{Si}(\text{C}_5\text{H}_4)_2\text{TiCl}_2]$ (13**):** A solution of $n\text{BuLi}$ (4.60 mL, 10.6 mmol in hexane) at 0°C was added to a solution of freshly distilled cyclopentadiene (0.88 mL, 10.6 mmol) in THF (30 mL). The mixture was stirred for 0.5 h at room temperature and then cooled to 0°C, $(\text{CH}_2)_4\text{SiCl}_2$ (0.07 mL, 5.3 mmol) was added. The mixture was stirred for 3 h at room temperature and then cooled to 0°C again; another portion of $n\text{BuLi}$ in hexane solution (4.60 mL, 10.6 mmol) was added. The mixture was stirred for 6 h at room temperature. A solution of $\text{TiCl}_4 \cdot 2\text{THF}$ (1.77 g, 5.3 mmol) in THF (20 mL) was added to the mixture, which was then stirred for 10 h at room temperature. The solvent was removed in vacuo and the residue was extracted with CH_2Cl_2 . Concentration and cooling of the CH_2Cl_2 solution afforded **13** as black crystals. Yield: 50 mg (3%); m.p. 198°C (decomp); ^1H NMR (CDCl_3 , 25°C): δ = 7.21 (m, 4H; C_5H_4), 5.96 (m, 4H; C_5H_4), 1.91 (m, 4H; SiCH_2), 1.25 ppm (m, 4H; CH_2); EI-MS (70 eV): m/z (%): 330 (32) [M^+], 295 (11) [$\text{M}^+ - \text{Cl}$], 294 (11) [$\text{M}^+ - \text{HCl}$], 258 (16) [$\text{M}^+ - 2\text{HCl}$], 211 (7) [$\text{M}^+ - \text{Cl} - (\text{CH}_2)_4\text{Si}$], 176 (100) [$\text{M}^+ - 2\text{Cl} - (\text{CH}_2)_4\text{Si}$], 150 (17), 93 (18), 83 (26); elemental analysis calcd (%) for $\text{C}_{14}\text{H}_{16}\text{Cl}_2\text{SiTi}$ (331.14): C 50.78, H 4.87; found: C 50.45, H 4.84.

Synthesis of $[(\text{CH}_2)_4\text{Si}(\text{C}_5\text{H}_4)_2\text{ZrCl}_2]$ (14**):** Synthesis of **14** from cyclopentadiene, $n\text{BuLi}$, $(\text{CH}_2)_4\text{SiCl}_2$, and $\text{ZrCl}_4 \cdot 2\text{THF}$ was similar to that described for **13**. Yellow powder; yield: 0.3 g (15.1%); m.p. 236°C (decomp); ^1H NMR (CDCl_3 , 25°C): δ = 6.96 (m, 4H; C_5H_4), 5.98 (m, 4H; C_5H_4), 1.90 (m, 4H; SiCH_2), 1.26 ppm (m, 4H; CH_2); EI-MS (70 eV): m/z (%): 374 (100) [$\text{M}^+ + 2$], 372 (93) [M^+], 336 (41) [$\text{M}^+ - \text{HCl}$], 253 (69) [$\text{M}^+ - \text{Cl} - (\text{CH}_2)_4\text{Si}$], 218 (72) [$\text{M}^+ - 2\text{Cl} - (\text{CH}_2)_4\text{Si}$], 93 (85); elemental analysis calcd (%) for $\text{C}_{14}\text{H}_{16}\text{Cl}_2\text{SiZr}$ (374.50): C 44.91, H 4.31; found: C 44.47, H 4.38.

Ethylene polymerization: Polymerizations were carried out in a 250-mL glass reactor with a magnetic stirring bar at about 780 mmHg. Toluene (100 mL) was introduced into the reactor, the temperature was raised to the polymerization temperature, then the toluene was saturated with ethylene. A prescribed amount of MAO and a given metallocene complex dissolved in toluene were injected into the reactor, then the polymerization was started. It was stopped by adding methanolic hydrochloric acid solution (100 mL). The polymer product was washed with ethanol and dried in vacuo at 60°C. Number- and weight-average molecular weights were obtained with a Waters 150C GPC instrument. The columns were calibrated with polyethylene standards.

X-ray crystallography: Crystals of **4–9** suitable for single-crystal X-ray analysis were obtained from CH_2Cl_2 /hexane solution. Data collection was performed on a Bruker Smart 1000 (**4**, **5**, **6**, **8**) or an Enraf-Nonius CAD-4 (**7**, **9**) diffractometer using graphite-monochromated MoK_α radiation and ω - 2θ scan. Empirical absorption corrections using the DIFBAS were applied for **7** and **9**, while semi-empirical absorption corrections were applied for **4**, **5**, **6**, and **8**. The structures were solved by direct methods and refined by full-matrix least-squares. For all calculations the SDP-PLUS, SHELXL-97, or Siemens SHELXTL-PC program system was used. Table 8 contains the crystal data and a summary of X-ray data collection details.

CCDC-212943 (**4**), CCDC-212944 (**5**), CCDC-212945 (**6**), CCDC-212946 (**7**), CCDC-212947 (**8**), and CCDC-212948 (**9**) contain the supplementary crystallographic data for this paper. These data can be obtained free of charge from The Cambridge Crystallographic Data Centre via www.ccdc.cam.ac.uk/data_request/cif.

Acknowledgement

This work was supported financially by the National Natural Science Foundation of China (29734142, 20202004), SINOPEC, the Scientific Research Foundation for Returned Overseas Chinese Scholars, the State

Table 8. Crystal data and summary of X-ray data collection

	4	5	6	7	8	9
formula	$\text{C}_{15}\text{H}_{16}\text{Cl}_2\text{Ti}$	$\text{C}_{16}\text{H}_{18}\text{Cl}_2\text{Ti}$	$\text{C}_{17}\text{H}_{20}\text{Cl}_2\text{Ti}$	$\text{C}_{15}\text{H}_{16}\text{Cl}_2\text{Zr}$	$\text{C}_{16}\text{H}_{18}\text{Cl}_2\text{Zr}$	$\text{C}_{17}\text{H}_{20}\text{Cl}_2\text{Zr}$
M_w [g mol $^{-1}$]	315.08	329.10	343.13	358.42	372.42	386.47
T [K]	293(2)	293(2)	293(2)	299(1)	293(2)	299(1)
crystal system	triclinic	monoclinic	triclinic	triclinic	monoclinic	triclinic
space group	$P\bar{1}$	$P2_1/c$	$P\bar{1}$	$P\bar{1}$	$P2_1/c$	$P\bar{1}$
a [Å]	0.71073	0.71073	0.71073	0.71073	0.71073	0.71073
b [Å]	7.262(2)	7.553(3)	7.535(3)	8.271(3)	7.606(5)	7.622(2)
c [Å]	8.122(3)	24.462(9)	8.392(3)	8.387(2)	25.187(17)	8.471(2)
α [°]	12.651(4)	8.225(3)	13.243(5)	11.018(2)	8.364(6)	13.468(3)
β [°]	78.910(5)	90	91.536(7)	70.15(2)	90	91.11(3)
γ [°]	73.362(5)	107.981(6)	103.090(6)	75.69(2)	108.412(9)	103.56(3)
χ [°]	72.733(5)	90	109.796(6)	81.64(2)	90	109.59(3)
V [Å 3]	678.0(4)	1445.4(9)	762.5(5)	695.0(1)	1520.4(18)	791.8(4)
Z	2	4	2	2	4	2
D_{calcd} [g cm $^{-3}$]	1.543	1.512	1.495	1.713	1.627	1.621
μ [mm $^{-1}$]	1.003	0.944	0.898	1.1453	1.058	1.0113
$F(000)$	324	680	356	360	752	392
crystal size [mm 3]	0.30 × 0.25 × 0.20	0.30 × 0.25 × 0.20	0.30 × 0.25 × 0.20	0.30 × 0.35 × 0.40	0.35 × 0.30 × 0.10	0.30 × 0.30 × 0.50
$2\theta_{\text{max}}$ [°]	50.06	50.06	50.04	50	50.04	50
measured reflections	2837	5880	3176	2120	6104	2894
unique reflections	2387	2538	2670	1937	2668	2731
observed reflections	2387	2538	2670	1792	2668	2565
$[I > 2\sigma(I)]$			$[I \geq 3\sigma(I)]$		$[I \geq 3\sigma(I)]$	
parameters	163	172	181	163	172	181
goodness-of-fit on F^2	1.007	1.117	1.051	1.23 (on F)	1.010	1.49 (on F)
R_1 , wR_2 [$I > 2\sigma(I)$]	0.0370, 0.0925	0.0435, 0.0887	0.0458, 0.1128	0.087, 0.086	0.0614, 0.1471	0.045, 0.052
R_1 , wR_2 (all data)	0.0495, 0.0979	0.0673, 0.0953	0.0713, 0.1301	$[I \geq 3\sigma(I)]$	0.0821, 0.1653	$[I \geq 3\sigma(I)]$
$\Delta\rho$ [e Å $^{-3}$]	0.410/−0.362	0.364/−0.340	0.697/−0.359	1.53/−1.02	0.725/−1.155	0.95/−1.22

Education Ministry (2001–345), and the State Key Laboratory of Organometallic Chemistry, Shanghai Institute of Organic Chemistry, Chinese Academy of Sciences.

- [1] a) *Transition Metals and Organometallics as Catalysts for Olefin Polymerization* (Eds.: W. Kaminsky, H. Sinn), Springer, Berlin, **1988**; b) W. Kaminsky, *Catal. Today* **1994**, *20*, 257–271; c) W. Kaminsky, M. Arndt, *Adv. Polym. Sci.* **1997**, *127*, 143–187; d) W. Kaminsky, *J. Chem. Soc. Dalton Trans.* **1998**, 1413–1418; e) *Metallocenes: Synthesis, Reactivity, Applications* (Eds.: A. Togni, R. L. Halterman), Wiley-VCH, Weinheim, **1998**.
- [2] a) H.-H. Brintzinger, D. Fischer, R. Mülhaupt, B. Rieger, R. M. Waymouth, *Angew. Chem.* **1995**, *107*, 1255–1283; *Angew. Chem. Int. Ed. Engl.* **1995**, *34*, 1143–1170; b) H. G. Alt, A. Köppl, *Chem. Rev.* **2000**, *100*, 1205–1221; c) L. Resconi, L. Cavallo, A. Fait, F. Piemontesi, *Chem. Rev.* **2000**, *100*, 1253–1345.
- [3] a) P. C. Möhring, N. J. Coville, *J. Organomet. Chem.* **1994**, *479*, 1–29; b) H. G. Alt, E. Samuel, *Chem. Soc. Rev.* **1998**, *27*, 323–329.
- [4] a) J. A. Smith, J. V. Seyerl, G. Huttner, H.-H. Brintzinger, *J. Organomet. Chem.* **1979**, *173*, 175–185; b) F. Wild, L. Zsolnai, G. Huttner, H.-H. Brintzinger, *J. Organomet. Chem.* **1982**, *232*, 233–247; c) F. Wild, M. Wasiucionek, G. Huttner, H.-H. Brintzinger, *J. Organomet. Chem.* **1985**, *288*, 63–67.
- [5] W. Kaminsky, K. Külper, H.-H. Brintzinger, F. R. W. P. Wild, *Angew. Chem.* **1985**, *97*, 507–508; *Angew. Chem. Int. Ed. Engl.* **1985**, *24*, 507–508.
- [6] a) W. Hermann, J. Rohrmann, E. Herdtweck, W. Spaleck, A. Winter, *Angew. Chem.* **1989**, *101*, 1536–1537; *Angew. Chem. Int. Ed. Engl.* **1989**, *28*, 1511–1512; b) T. Mise, S. Miya, H. Yamazaki, *Chem. Lett.* **1989**, 1853–1856; c) W. Spaleck, M. Antberg, J. Rohrmann, A. Winter, B. Bachmann, P. Kiprof, J. Behm, W. A. Herrmann, *Angew. Chem.* **1992**, *104*, 1373–1376; *Angew. Chem. Int. Ed. Engl.* **1992**, *31*, 1347–1350; d) W. Spaleck, F. Kuber, A. Winter, J. Rohrmann, B. Bachmann, M. Antberg, V. Dolle, E. F. Paulus, *Organometallics* **1994**, *13*, 954–963; e) *Ziegler Catalysts* (Eds.: R. Mülhaupt, H.-H. Brintzinger), Springer, Berlin, **1995**; f) *Metalorganic Catalysts for Synthesis and Polymerization* (Ed.: W. Kaminsky), Springer, Berlin, **1999**; g) J. C. Green, *Chem. Soc. Rev.* **1998**, *27*, 263–271.
- [7] P. J. Shapiro, *Coord. Chem. Rev.* **2002**, *231*, 67–81.
- [8] a) X. Zhou, B. Wang, S. Xu, *Chem. J. Chinese Univ.* **1995**, *16*, 887–891; b) B. Wang, X. Zhou, S. Xu, N. Hu, *Chem. J. Chinese Univ.* **1996**, *17*, 231–235; c) B. Wang, S. Xu, X. Zhou, L. Su, R. Feng, D. He, *Chem. J. Chinese Univ.* **1999**, *20*, 77–80; d) X. Sun, B. Wang, S. Xu, X. Zhou, J. Zhao, Y. Hu, *Chem. J. Chinese Univ.* **2000**, *21*, 222–226; e) S. Xu, G. Tian, B. Wang, X. Zhou, B. Liang, L. Zhao, *Chem. J. Chinese Univ.* **2002**, *23*, 595–599; f) S. Xu, T. Wu, H. Cui, B. Wang, X. Zhou, F. Zou, Y. Li, *Chem. J. Chinese Univ.* **2002**, *23*, 1891–1895; g) B. Wang, L. Su, S. Xu, R. Feng, X. Zhou, D. He, *Macromol. Chem. Phys.* **1997**, *198*, 3197–3205; h) G. Tian, B. Wang, S. Xu, Y. Zhang, X. Zhou, *J. Organomet. Chem.* **1999**, *579*, 24–29; i) G. Tian, B. Wang, X. Dai, S. Xu, X. Zhou, J. Sun, *J. Organomet. Chem.* **2001**, *634*, 145–152; j) S. Xu, X. Dai, B. Wang, X. Zhou, *J. Organomet. Chem.* **2002**, *645*, 262–267.
- [9] S. Xu, X. Deng, B. Wang, X. Zhou, L. Yang, Y. Li, Y. Hu, F. Zou, Y. Li, *Macromol. Rapid Commun.* **2001**, *22*, 708–709.
- [10] I. E. Nifant'ev, P. V. Ivchenko, M. V. Borzov, *J. Chem. Res. Synop.* **1992**, 162.
- [11] R. M. Shaltout, J. Y. Corey, N. P. Rath, *J. Organomet. Chem.* **1995**, *503*, 205–212.
- [12] A. Clearfield, D. K. Warner, C. H. Saldarriaga-Molina, R. Ropal, I. Bernal, *Can. J. Chem.* **1975**, *53*, 1622–1629.
- [13] a) K. Prout, T. S. Cameron, R. A. Forder, *Acta Crystallogr. Sect. B* **1974**, *30*, 2290–2304; b) J. Y. Corey, X.-H. Zhu, L. Brammer, N. P. Rath, *Acta Crystallogr. Sect. C* **1995**, *51*, 565–567.
- [14] a) I. E. Nifant'ev, P. V. Ivchenko, V. V. Bagrov, L. G. Kuz'mina, *Organometallics* **1998**, *17*, 4734–4738; b) C. A. Willoughby, W. M. Davis, S. L. Buchwald, *J. Organomet. Chem.* **1995**, *497*, 11–15.
- [15] C. S. Bajgur, W. R. Tikkanen, J. L. Petersen, *Inorg. Chem.* **1985**, *24*, 2539–2546.
- [16] a) J. A. Ewen, *J. Am. Chem. Soc.* **1984**, *106*, 6355–6364; b) J. A. Ewen, L. Haspeslagh, *J. Am. Chem. Soc.* **1987**, *109*, 6544–6545; c) M. L. H. Green, N. Ishihara, *J. Chem. Soc. Dalton Trans.* **1994**, 657–665.
- [17] a) W. Kaminsky, *Catal. Today* **1994**, *20*, 257–271; b) S. Miyake, Y. Okumura, S. Inazawa, *Macromolecules*, **1995**, *28*, 3074–3079; c) G. Erkers, C. Psiorz, R. Fröhlich, M. Grehl, C. Krüger, R. Noe, M. Noite, *Tetrahedron* **1995**, *51*, 4347–4358; d) J. A. Ewen, A. Zambelli, P. Longo, J. M. Sullivan, *Macromol. Rapid Commun.* **1998**, *19*, 71–73; e) M. H. Lee, Y. Han, D.-H. Kim, J.-W. Hwang, Y. Do, *Organometallics* **2003**, *22*, 2790–2796; f) E. Polo, S. Losio, F. Fortini, P. Locatelli, M. C. Sacchi, *Macromol. Symp.* **2004**, *213*, 89–99.
- [18] S.-J. Kim, Y.-J. Lee, E. Kang, S. H. Kim, J. Ko, B. Lee, M. Cheong, I.-H. Suh, S. O. Kang, *Organometallics* **2003**, *22*, 3958–3966.
- [19] R. F. Jordan, R. E. Lapointe, N. Baenziger, G. D. Hinch, *Organometallics* **1990**, *9*, 1539–1545.
- [20] a) L. Resconi, F. Piemontesi, I. Camurati, O. Sudmeijer, I. E. Nifant'ev, P. V. Ivchenko, L. G. Kuz'mina, *J. Am. Chem. Soc.* **1998**, *120*, 2308–2321; b) L. Resconi, D. Balboni, G. Baruzzi, C. Fiori, S. Guidotti, *Organometallics* **2000**, *19*, 420–429.
- [21] W. Kaminsky, R. Engehausen, K. Zoumis, W. Spaleck, J. Rohrmann, *Makromol. Chem.* **1992**, *193*, 1643–1651.
- [22] a) G. H. Llinas, R. O. Day, M. D. Rausch, J. C. W. Chien, *Organometallics* **1993**, *12*, 1283–1288; b) D. T. Mallin, M. D. Rausch, G.-Y. Lin, S. Dong, J. C. W. Chien, *J. Am. Chem. Soc.* **1990**, *112*, 2030–2031; c) J. C. W. Chien, G. H. Llinas, M. D. Rausch, G.-Y. Lin, H. H. Winter, *J. Am. Chem. Soc.* **1991**, *113*, 8569–8570; d) J. C. W. Chien, G. H. Llinas, M. D. Rausch, G.-Y. Lin, H. H. Winter, *J. Polym. Sci. Part A* **1992**, *30*, 2601–2617.
- [23] L. Manzer, *Inorg. Synth.* **1982**, *21*, 135–138.
- [24] R. West, *J. Am. Chem. Soc.* **1954**, *76*, 6012–6014.
- [25] E. Gianetti, G. M. Nicoletti, R. Mazzocchi, *J. Polym. Sci. Part A* **1985**, *23*, 2117–2134.

Received: July 21, 2004
Published online: December 2, 2004